Balance of Pro- and Anti-Inflammatory Cytokines Correlates with Outcome of Acute Experimental *Pseudomonas aeruginosa* Keratitis

A. Thakur,[1]* M. Xue,[1] F. Stapleton,[1] A. R. Lloyd,[2] D. Wakefield,[2] and M. D. P. Willcox[1]

Cornea and Contact Lens Research Unit, Cooperative Research Centre for Eye Research and Technology,[1] and Inflammation Research Unit, School of Pathology,[2] The University of New South Wales, Sydney, New South Wales 2052, Australia

The purpose of this study was to elucidate the expression of pro- and anti-inflammatory cytokines in mouse corneas infected with *Pseudomonas aeruginosa*. Three bacterial strains (invasive, cytotoxic, or CLARE [contact lens-induced acute red eye]) which have recently been shown to produce distinct patterns of corneal disease in the mouse were used. The left mouse (BALB/c) corneas were scarified and infected with 2×10^6 CFU of one of the three *P. aeruginosa* strains, while right eyes served as controls. Animals were examined at 1, 4, 8, 16, and 24 h with a slit lamp biomicroscope to grade the severity of infection. Following examination, eyes were collected and processed for histopathology, multiprobe RNase protection assay for cytokine mRNA, enzyme-linked immunosorbent assay to quantitate cytokine proteins, and myeloperoxidase activity to quantitate polymorphonuclear leukocytes. The kinetics of appearance and magnitude of expression of key cytokines varied significantly in the three different phenotypes of *P. aeruginosa* infection. The predominant cytokines expressed in response to all three phenotypes were interleukin-1β (IL-1β), IL-1Ra, and IL-6. In response to the invasive strain, which induced severe corneal inflammation, significantly lower ratios of IL-1Ra to IL-1β were present at all time points, whereas corneas challenged with the CLARE strain, which induced very mild inflammation, showed a high ratio of IL-1Ra to IL-1β. The outcome of infection in bacterial keratitis correlated with the relative induction of these pro- and anti-inflammatory cytokines, and exogenous administration of recombinant rIL-1Ra (rIL-1Ra) was able to reduce the disease severity significantly. These findings point to the therapeutic potential of rIL-1Ra protein in possible treatment strategies for bacterial keratitis.

Keratitis induced by *Pseudomonas aeruginosa* is a potentially devastating corneal inflammatory disease that may lead to permanent vision loss from progressive destruction of the cornea or from scarring. The key contributing factors for bacterial keratitis include compromised immunity, trauma, and contact lens wear. Corneal infection in humans with *P. aeruginosa* is commonly characterized by rapid infiltration of polymorphonuclear leukocytes (PMNs), corneal ulceration, and various degrees of stromal destruction (29, 52). These outcomes may result from the effects of host factors as well as tissue-destructive bacterial enzymes (30, 31, 47). Although rapid infiltration of PMNs is required to eliminate the infecting bacteria, the continued presence of PMNs, implying ongoing inflammation, appears to promote corneal damage and scarring (7).

The induction of acute inflammation is regulated by proinflammatory cytokines which can be induced in response to the lipopolysaccharide component of gram-negative bacteria and by host response factors. In the context of bacterial keratitis, expression of proinflammatory cytokines, such as interleukin-1β (IL-1β), IL-6, and tumor necrosis factor alpha (TNF-α), may contribute directly or indirectly to corneal ulceration by promoting the recruitment and activation of PMNs and by induction of tissue-damaging enzymes (24, 37, 43, 55). Human and mouse corneal tissues, including epithelium and stromal keratocytes, express IL-1, IL-1Ra, TNF-α, and IL-6 mRNA and protein both in vitro and in vivo (8, 11, 28, 32, 44) in

response to bacteria or proinflammatory cytokines. Our previous studies have demonstrated the presence of proinflammatory cytokines in human tears collected during eye closure and in inflammatory responses such as contact lens-induced acute red eye (CLARE) (49–51). More recently, Rudner et al. (45) have shown that down-regulation of IL-1β in a mouse model of *Pseudomonas* keratitis may expedite the clearance of bacteria and recovery from corneal disease.

In this study three phenotypes of *P. aeruginosa* which have recently been shown to produce distinct patterns of corneal disease in mice were used (9). The invasive and cytotoxic phenotypes of *P. aeruginosa* appear to be mutually exclusive, and this exclusivity has been shown to be dependent on possession of a number of genes. Invasive strains possess the genes *exoS* and *exoT*, which encode the ADP-ribosylating toxins ExoS and ExoT, respectively (22, 23). Cytotoxic strains possess only the gene *exoT* (23). The names cytotoxic and invasive refer to the interactions between epithelial cells and the bacteria (20). The cytotoxic strains cause a rapid cytotoxicity in the mammalian cells, whereas the invasive strains can remain inside cells for up to 24 h before the cells show any overt cytopathic effect (21). While both cytotoxic and invasive strains can produce large amounts of proteases (10, 22), the CLARE strain can produce only low levels (10, 18). The invasive and cytotoxic strains were isolated from human microbial keratitis. The CLARE strain (Paer1) is not associated with tissue destruction in the cornea but causes the self-limiting condition known as CLARE (10).

The present study was undertaken to investigate the complexity of corneal responses to bacterial infection with these three distinct strains of *P. aeruginosa*. The hypothesis underly-

* Corresponding author. Present address: Department of Anatomy and Cell Biology, School of Medicine, Wayne State University, 540 E. Canfield Ave., Detroit, MI 48201. Phone: (313) 577-1074. Fax: (313) 577-3125. E-mail: a.thakur@med.wayne.edu.

TABLE 1. Anterior segment variables used for corneal disease scoring

Score	Description				
	Corneal infiltrates			Epithelial defects	
	Density	Depth (% of stromal thickness)	Extent (% of corneal area)	Defect size (mm)	Depth (% of epithelial thickness)
0	None	No infiltrates	No infiltrates	None	No defect
1	Very slight (iris visible)	5–20	5–20	0.1–1.0	5–20
2	Slight (iris partly obscured)	30–40	30–40	1.1–2.0	30–40
3	Moderate (iris not visible)	50–70	50–70	2.1–3.0	50–70
4	Severe (opaque)	70–100	70–100	3.1–4.0	70–100

ing this work was that three different strains of *P. aeruginosa*, which have been shown to produce distinct pathologies during initial stages of infection in mouse eyes and which were isolated from two distinct clinical conditions in humans eyes, will produce different levels of proinflammatory and anti-inflammatory cytokines (IL-1β, TNF-α, IL-1Ra, IL-6, and IL-10).

MATERIALS AND METHODS

Animal model. BALB/c mice 8 to 10 weeks old were used in this study. All mice were subjected to baseline measurements of corneal integrity, including slit lamp evaluation. Details of tear film, corneal transparency, hyperemia, and anterior chamber status were assessed, and only those animals which were in the normal range for these clinical variables were used in the study. The Association for Research in Vision and Ophthalmology guidelines on the use of animals in experimentation were adhered to, and appropriate institutional ethics clearance was obtained.

Bacterial strains and growth conditions. Three bacterial strains (*P. aeruginosa* strains Paer1, 6206, and 6294) were used. Bacterial cells from each strain were grown in 10 ml of tryptone soy broth (Oxoid Ltd., Sydney, Australia) overnight at 37°C. Bacteria were harvested, washed three times in sterile phosphate-buffered saline (PBS) (pH 7.4), and resuspended in PBS at an infecting dose (9) of 4×10^8 cells/ml (optical density at 660 nm of 0.5).

Animal infection. Both corneas of each animal were scarified by using a 26-gauge needle under a stereomicroscope (two parallel incisions of 2 mm in length and 3 to 4 layers of epithelium in depth, randomly confirmed by histological evaluation). Fourteen animals were included at each time point (three eyes for histology, three for PMN enumeration, three for enzyme-linked immunosorbent assay [ELISA], and five for RNA studies) for each bacterial strain. All experiments were repeated at least twice. The left-side corneas were challenged topically with 2×10^6 live bacteria (*P. aeruginosa*) in a 5-μl dose, while the right-side corneas received 5 μl of PBS.

Administration of IL-1Ra. Mouse recombinant IL-1Ra (rIL-1Ra) was purchased from R & D Systems, Minneapolis, Minn. The lyophilized protein was reconstituted and diluted to a concentration of 10 μg/10 μl. Anesthetized animals were injected with 20 μl of rIL-1Ra (20 μg during each injection) subconjunctivally 24 h and then 3 h before infection. Control mice received an equal volume of PBS at the same time points. Both IL-1Ra- and PBS-treated animals were challenged with the invasive strain of *P. aeruginosa*. These experiments were repeated three times.

Clinical examination. Anesthetized animals were examined at 1, 4, 8, 16, and 24 h and 3, 5, and 7 days with a slit lamp biomicroscope to grade the severity of infection, using the anterior segment variables presented in Table 1. A composite corneal disease score was derived from the sum of the five variables in Table 1 (the maximum total score would be 20 [maximum grade of 4×5 variables]). The severity of edema was also graded as 0 to 4, where 1 corresponds to no edema, 1 to very slight edema, 2 to slight edema, 3 to moderate edema, and 4 to severe edema (bullae). Neovascularization was noted as extent (millimeters) from the limbus.

Histopathology of mouse corneas. At various time intervals (1, 4, 8, 16, and 24 h and 3, 5, and 7 days), animals were sacrificed before eyes were removed and fixed in 2.5% glutaraldehyde in PBS (pH 7.4) at 4°C for 4 h. After fixation, the tissues were washed three times with PBS and then dehydrated in graded ethanol solutions. Tissues were left in the infiltrating solution for at least 1 day before embedding in Histo-resin plus (Leica, Heidelberg, Germany). Tissue sections of 5 μm in thickness were stained with toluidene blue and examined under light

microscopy for the presence of infiltrating leukocytes, epithelial defects, and stromal melting.

Measurement of MPO activity. Ocular myeloperoxidase (MPO) activity was determined by a method described previously (56). Briefly, whole eyes were homogenized in 1 ml of hexadecyl trimethylammonium bromide buffer (0.5% hexadecyl trimethylammonium bromide in 50 mM phosphate buffer, pH 6.0) and sonicated for 10 s in an ice bath. The samples were freeze-thawed three times and centrifuged at $12,000 \times g$ for 20 min. The supernatant (0.1 ml) was mixed with 2.9 ml of 50 mM phosphate buffer (pH 6.0) containing 0.167 mg of *O*-dianisidine hydrochloride per ml and 0.0005% hydrogen peroxide. The change in absorbance at 460 nm was continuously monitored for 5 min. Three eyes were used each time point, and measurements were repeated at least two times. One unit of MPO activity was determined to be equivalent to approximately 2×10^5 PMNs/ml (56).

Cytokine protein determination by ELISA. Cytokine levels were measured in homogenates of control and challenged eyes at different time points by using ELISA kits (R & D Systems) or in-house ELISAs. Samples for ELISA were prepared by homogenizing the whole mouse eye in sterile PBS. Homogenates were centrifuged at $4,000 \times g$ for 20 min at 4°C. The resulting supernatants were used to quantitate TNF-α, IL-1β, IL-6, IL-1Ra, and IL-10 proteins. Supernatants, diluted 1:5 in the sample diluting buffer, were added in duplicate wells. Samples were analyzed according to the manufacturer's instructions.

RNase protection assay. Whole eyes (five) were homogenized in Tri-solution (Sigma-Aldrich, Sydney, Australia), and total RNA was purified. RNA was isolated by phenol-chloroform extraction and ethanol precipitation, resuspended in RNase-free water, and quantitated by measuring absorbance at 260 nm. A multiprobe RNase protection assay (Pharmingen, Sydney, Australia) was used to measure cytokine (TNF-α, IL-1β, IL-6, IL-1Ra, and IL-10) mRNAs. Briefly, a mixture of ^{32}P-labeled antisense riboprobes was generated from a cDNA template. Total RNA isolated from mouse eyes was hybridized with ^{32}P-labeled riboprobe at 56°C overnight. After completion of hybridization, the samples were digested with T_1 nuclease and proteinase K. Protected fragments were purified by phenol-chloroform extraction followed by ethanol precipitation. Protected hybridized RNA samples were air dried and reconstituted in 2 μl of loading buffer. These samples were resolved on a 4.5% polyacrylamide sequencing gel. After separation of fragments, the gel was transferred to filter paper, dried, and exposed to X-ray film (Kodak X-Omat; Sigma Chemical Co., St Louis, Mo.) overnight at −70°C. The film was developed, and bands were identified by measuring molecular masses. Relative quantities were determined using Multianalyst software (Bio-Rad, Sydney, Australia). Induction of cytokine mRNAs was expressed as relative density normalized to the internal control (GAPDH [glyceraldehyde-3-phosphate dehydrogenase]).

Statistical analysis. Statistical analysis of data was performed by using one-way analysis-of-variance tests to assess the differences in cytokine mRNA and protein expression in the infected corneas. In addition, Pearson's correlations between indices of disease severity (the composite corneal score, edema, and neovascularization) and the ratio of IL-1β to IL-1Ra, as well as the levels of IL-6, at 1, 3, 5, and 7 days postchallenge were sought. For the purpose of this analysis, it was assumed that direct microbial contributions to pathogenesis were equivalent in all three bacterial strains; therefore, host variables that determine phenotype were sought.

RESULTS

The host response to three phenotypes of *P. aeruginosa* was determined by using clinical and histological examination, neu-
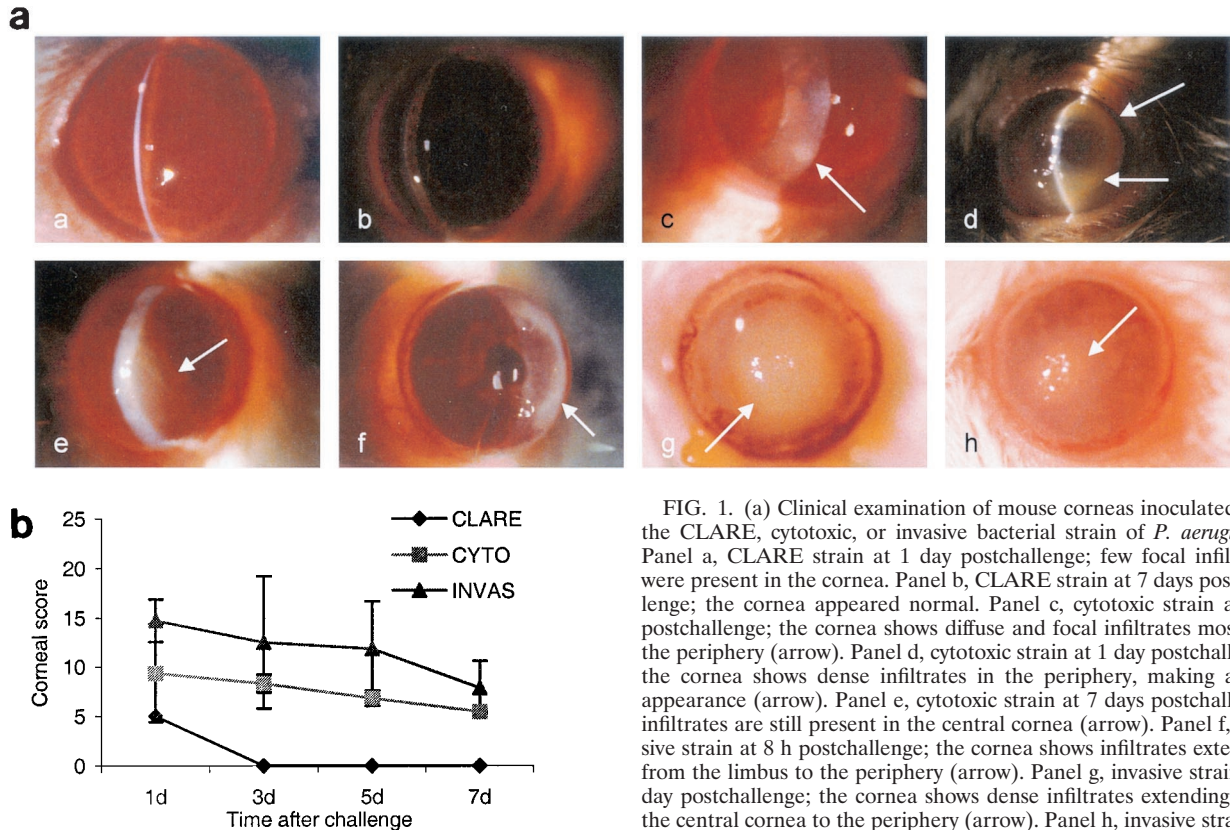
a

b

FIG. 1. (a) Clinical examination of mouse corneas inoculated with the CLARE, cytotoxic, or invasive bacterial strain of *P. aeruginosa*. Panel a, CLARE strain at 1 day postchallenge; few focal infiltrates were present in the cornea. Panel b, CLARE strain at 7 days postchallenge; the cornea appeared normal. Panel c, cytotoxic strain at 8 h postchallenge; the cornea shows diffuse and focal infiltrates mostly in the periphery (arrow). Panel d, cytotoxic strain at 1 day postchallenge; the cornea shows dense infiltrates in the periphery, making a ring appearance (arrow). Panel e, cytotoxic strain at 7 days postchallenge; infiltrates are still present in the central cornea (arrow). Panel f, invasive strain at 8 h postchallenge; the cornea shows infiltrates extending from the limbus to the periphery (arrow). Panel g, invasive strain at 1 day postchallenge; the cornea shows dense infiltrates extending from the central cornea to the periphery (arrow). Panel h, invasive strain at: 7 days postchallenge; the corneal pathology had resolved somewhat (arrow shows infiltrates). (b) Composite clinical scores (composed of the graded density, depth, and extent of corneal infiltrates as well as size and depth of corneal ulceration; see Table 1 for the grading system) for corneas challenged with the invasive (INVAS), cytotoxic (CYTO), and CLARE bacterial strains. Error bars indicate standard errors of the means.

trophil infiltration (MPO activity) of the cornea, and cytokine assays.

Clinical examination. Mice were examined at 1, 4, 8, 16, and 24 h and 3, 5, and 7 days with a slit lamp biomicroscope to grade the severity of infection by using the anterior segment variables presented in Table 1. For each time point, eight animals were subjected to clinical examination. Mouse corneas inoculated with the CLARE strain showed a visible scratch site but no infiltrates at 4 h postinoculation. By 8 h the scratch site had healed in all animals, and only isolated focal infiltrates (grade, 1) were observed (Fig. 1a, panel a). After 24 h, sparse focal infiltrates were present, but there was no anterior chamber response or epithelial defect (Fig. 1a, panel b). By day 7 postchallenge, corneas had completely recovered.

Corneas inoculated with the cytotoxic strain showed infiltrates in a single diffuse patch at 4 h postchallenge, with a visible scratch site. After 8 h, multiple focal lesions had appeared either at the scratch site or at the periphery of the cornea (Fig. 1a, panel c). At this time point, the anterior chamber response was mild, and the scratch site had not healed in the majority of animals. At 24 h postchallenge, the cornea was markedly edematous (grade, 2.5 ± 0.5). Infiltrates covered 50 to 75% (grade, 2.4 ± 1.2) of the corneal diameter, and 50 to 75% (2.5 ± 1.3) of the stroma was involved. Only a small epithelial defect was present (0.6 ± 0.5 mm) at 24 h, notably smaller than that with the invasive strain. This ulceration involved 25% (grade, 1.4 ± 1.1) of the corneal thickness. The anterior chamber response and conjunctival injection were mild to moderate, again less prominent than in the invasive

strain (Fig. 1a, panel d). The composite score (9.4 ± 5) (Fig. 1b) for corneal inflammation was significantly lower (*P* < 0.005) than that for corneas inoculated with the invasive strain (14.7 ± 2) (Fig. 1b). Clinical examination on day 3 showed no significant difference in clinical score compared to day 1 postchallenge, except that there was slight neovascularization (extent, 0.1 ± 0.2 mm). On day 5, the clinical score was reduced significantly compared to that at day 1 postchallenge (*P* < 0.035). By day 7 corneas had recovered significantly, with an overall severity score of 5.4 ± 0.8 (Fig. 1a, panel e).

Corneas inoculated with the invasive strain showed diffuse leukocytic infiltrates by 4 h postchallenge, with a visible scratch site. At 8 h postchallenge infiltrates appeared at the periphery of the cornea (Fig. 1a, panel f). At this time point there was a mild anterior chamber response, and the scratch site had healed in approximately 50% of animals. Dramatic corneal inflammation was observed by 24 h, with severe ulceration and large central leukocytic infiltrates covering 75 to 100% (grade, 3.2 ± 0.7) of the corneal diameter, and with 100% (grade, 4) stromal involvement. Epithelial defects were present (1.2 ± 0.6 mm), notably unassociated with the scratch site. This ulceration involved 50 to 75% (grade, 2.8 ± 1.07) of the corneal thickness. There was a marked anterior chamber response, and
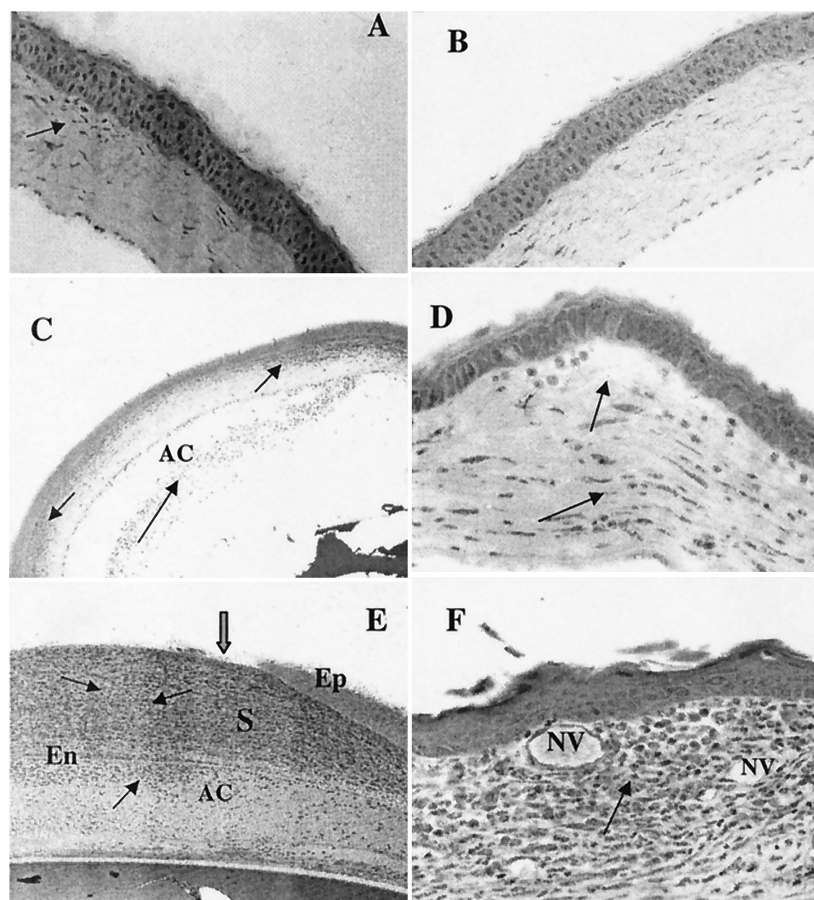
FIG. 2. Histological examination of mouse corneas at 1 and 7 days postchallenge. (A) Cornea inoculated with the CLARE strain showed focal infiltrates over the anterior corneal stroma (arrow). The initial scratch site was healed completely within 24 h of challenge. (B) At 7 days postchallenge with the CLARE strain, the cornea appeared to be completely normal. (C) Corneas inoculated with the cytotoxic strain also showed massive PMN infiltration, with leukocytes streaming through limbus and conjunctiva into the periphery of the corneal stroma (arrow) and to a lesser extent in the central cornea. Infiltrating cells were also present in anterior chamber (arrow). (D) At 7 days postchallenge with the cytotoxic strain, the cornea showed infiltrates in the central region (arrow) and less so in the peripheral cornea. The epithelium had completely healed by this time point. Stromal destruction was evident in the cornea as a result of extracellular matrix destruction, appearing as large white space (arrow). (E) Corneas inoculated with the invasive bacterial strain showed massive PMN infiltration (arrows) into the central stroma at 24 h postchallenge. The epithelium in the central cornea was completely destroyed (thick arrow). Large numbers of infiltrating cells were also present in the anterior chamber (arrow). (F) At 7 days postchallenge, the corneal epithelium was healed but infiltrates were still present (arrow) and new vessel growth was evident in the mid-periphery of the cornea. Ep, epithelium; S, stroma; En, endothelium; AC, anterior chamber; NV, new blood vessels.

conjunctival injection was prominent (Fig. 1a, panel g). Clinical examination on day 3 showed a prominent edematous response (grade, 3.5 ± 0.5) and the presence of neovascularization (extent, 0.1 mm from limbus). There was no significant difference in the composite clinical score on day 3 compared to day 1 postchallenge. By day 5, the overall clinical score had reduced significantly ($P < 0.024$) compared to day 1, but there was a significant ($P < 0.001$) increase in neovascularization (extent, 0.5 mm). At day 7 postchallenge, corneas had further recovered in all parameters compared to day 5 postchallenge ($P < 0.003$); however, the extent of neovascularization increased significantly compared to day 5 ($P < 0.001$) (Fig. 1a, panel h).

Histological examination. Eyes were enucleated at various time intervals (1, 4, 8, 16, and 24 h and 3, 5, and 7 days) following sacrifice and infection and processed for histopathological examination in response to three phenotypes of *P. aeruginosa*. Corneas inoculated with the CLARE strain

showed complete reepithelization at the scratch site, and very few infiltrates in the corneal stroma, at 8 h postchallenge. At 24 h postchallenge, sparse focal infiltrates were seen in the corneal stroma. The endothelium was intact and no anterior chamber response was evident at 24 h postchallenge. The epithelium at the initial scratch site was healed completely within 24 h of challenge (Fig. 2A). At 7 days postchallenge, the corneas appeared to be completely normal (Fig. 2B).

In mouse corneas challenged with the cytotoxic strain, PMNs were seen within 8 h around the scratch site, and bacteria were evident in the corneal stroma. After 24 h, numerous PMNs were apparent in the periphery of the corneal stroma and to a lesser extent in the central cornea. This was consistent with the macroscopic clinical finding of a broad ring appearance formed by infiltrates (Fig. 2C). On day 3, these infiltrates had extended into the central corneal stroma, in addition to dense infiltrates which were still evident at the periphery of the corneal stroma as well as in the anterior chamber. At this time

point, growth of a limited numbers of new vessels was apparent. On day 5 postchallenge, the infiltrating PMNs were less dense at the periphery of the cornea than at 1 day postchallenge. By day 7, the epithelium was completely healed, although infiltrating leukocytes were still abundant. Stromal destruction was also evident (Fig. 2D).

Histopathological examination of mouse corneas at 8 h postchallenge with the invasive strain revealed PMNs infiltrating from the limbus. Bacteria were evident in the anterior portion of the corneal stroma. At 24 h, there was a massive infiltration of PMNs, with cells streaming through the limbus and conjunctiva into the central stroma, consistent with the clinical findings described above. Bacteria were evident throughout the stroma, with denuded stroma apparent in the central cornea. The PMNs were aligned along Descemet's membrane, and the corneal stroma was markedly edematous (Fig. 2E). On day 3, the corneal histology remained essentially the same as on day 1, with large numbers of PMNs evident in the corneal stroma and anterior chamber. The epithelium had partially healed at the periphery of the defect. New vessel growth and marked edema were seen in the corneal stroma. On day 5 postchallenge, the density of infiltrating PMNs was reduced compared to that at 1 day postchallenge, but new blood vessels had extended toward the periphery of the cornea. By day 7, the epithelium was healed in the central cornea. New vessel formation was evident ((Fig. 2F). Large spaces had formed in the corneal stroma as a result of extracellular matrix destruction.

Neutrophil infiltration in the cornea. MPO activity was assayed to quantify the PMN infiltration in the whole mouse eye at 1, 4, 8, 16, and 24 h and 3, 5, and 7 days after challenge with each of the three *P. aeruginosa* strains. Corneas inoculated with the CLARE strain showed significant differences only at 16 h ($P < 0.03$) and 24 h ($P < 0.02$) postchallenge compared to scratch controls. Therefore, statistical comparisons were made between results with the CLARE strain and with the invasive or cytotoxic strains. High levels of MPO activity were observed in the corneas inoculated with the invasive ($P < 0.001$) or cytotoxic ($P < 0.03$) strains as early as 8 h postchallenge compared to CLARE strain-inoculated corneas. Corneas infected with the invasive or cytotoxic strains showed peak MPO activity at 24 h postchallenge, which remained high up to 3 days and declined significantly (invasive strain, $P = 0.0001$; cytotoxic strain, $P = 0.0001$) at 5 days compared to 24 h postchallenge (Fig. 3).

Evidence of differential cytokine mRNA expression after ocular challenge with *P. aeruginosa* strains. Cytokine mRNA expression in ocular homogenates in response to the three phenotypes of *P. aeruginosa* was measured at different time points (1, 4, 8, 16, and 24 h and 3, 5, and 7 days) by using a multiprobe RNase protection assay. In the CLARE strain-inoculated corneas, transcripts of IL-1β and IL-6 peaked at 8 h postchallenge. IL-1β expression declined substantially at 24 h postchallenge, while IL-6 remained at similar levels. IL-1Ra mRNA was present in low levels early during the infection but showed a marked increase at 24 h to 3 days postchallenge (Fig. 4a).

In corneas infected with the cytotoxic strain, transcripts of IL-1β were expressed as early as 1 h after the challenge, reached a plateau between 8 and 16 h postchallenge, and declined at 24 h postchallenge. IL-1Ra mRNA levels plateaued
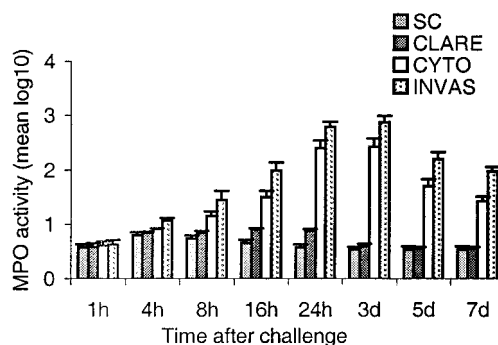

FIG. 3. MPO activity in whole eyes challenged with the invasive (INVAS), cytotoxic (CYTO), or CLARE strain and in a scratch control (SC) at 1, 4, 8, 16, and 24 h and 3, 5, and 7 days postchallenge. Results are reported as mean ($\pm$ standard error of the mean) $\log_{10}$ MPO activity/eye. Note that the horizontal axis is not on a linear scale.

between 24 h and 3 days postchallenge. Unlike the invasive strain, the cytotoxic strain induced significantly higher levels ($P < 0.04$) of IL-6 mRNA between 8 and 16 h postchallenge.

Transcripts for IL-1β were induced very early (1 h) in the cornea after the challenge with the invasive strain and peaked at 16 h postchallenge. IL-1Ra expression showed a slower pattern of induction, with peak levels at 24 h postchallenge. IL-6 mRNA was induced within 4 h postchallenge and remained elevated until 3 days postchallenge (Fig. 4a). TNF-α and IL-10 mRNAs were expressed only at low levels at all time points in response to all three strains (data not shown).

Evidence of differential cytokine protein expression after ocular challenge with *P. aeruginosa* strains. The examination of cytokine proteins was done by ELISA at various time points after infection of the cornea by three phenotypes of *P. aeruginosa*. High levels of IL-1Ra were detected in normal eyes (unscratched and uninfected). Cytokine expression in the CLARE strain-inoculated corneas showed continuous increases in IL-1β, IL-1Ra, and IL-6 proteins, reaching peak levels at 24 h after the challenge. The levels of IL-1β were significantly lower than those for invasive and cytotoxic strains ($P = 0.0001$ and $P = 0.003$, respectively). IL-6 protein levels were significantly higher ($P = 0.02$) than those for the invasive strain and significantly lower ($P = 0.004$) than those for the cytotoxic strain (Fig. 4b).

In response to the cytotoxic bacterial strain, peak levels of IL-1β and IL-6 were reached at 16 h postinfection and diminished by 24 h postchallenge, whereas the invasive strain-inoculated corneas showed peak levels at 24 h postinfection. The corneas inoculated with the cytotoxic strain showed significantly lower protein levels of IL-1β (8 h, $P = 0.0001$; 24 h, $P = 0.0001$; day 3, $P = 0.0001$) and IL-1Ra (8 h, $P = 0.001$; 24 h, $P = 0.001$; day, 3 $P = 0.0001$) than corneas inoculated with the invasive strain. Levels of IL-6 were significantly higher (8 h, $P = 0.0001$; 24 h, $P = 0.044$; day 3, $P = 0.02$) at all time points than those in the invasive strain-inoculated corneas (Fig. 4b).

The magnitude and kinetics of IL-1β, IL-1Ra, and IL-6 protein production in response to the invasive strain were significantly different from those in response to the cytotoxic and CLARE strains. The corneas inoculated with the invasive strain showed peak levels of most cytokine proteins at 24 h postinfection. IL-1β protein increased continuously from 8 to
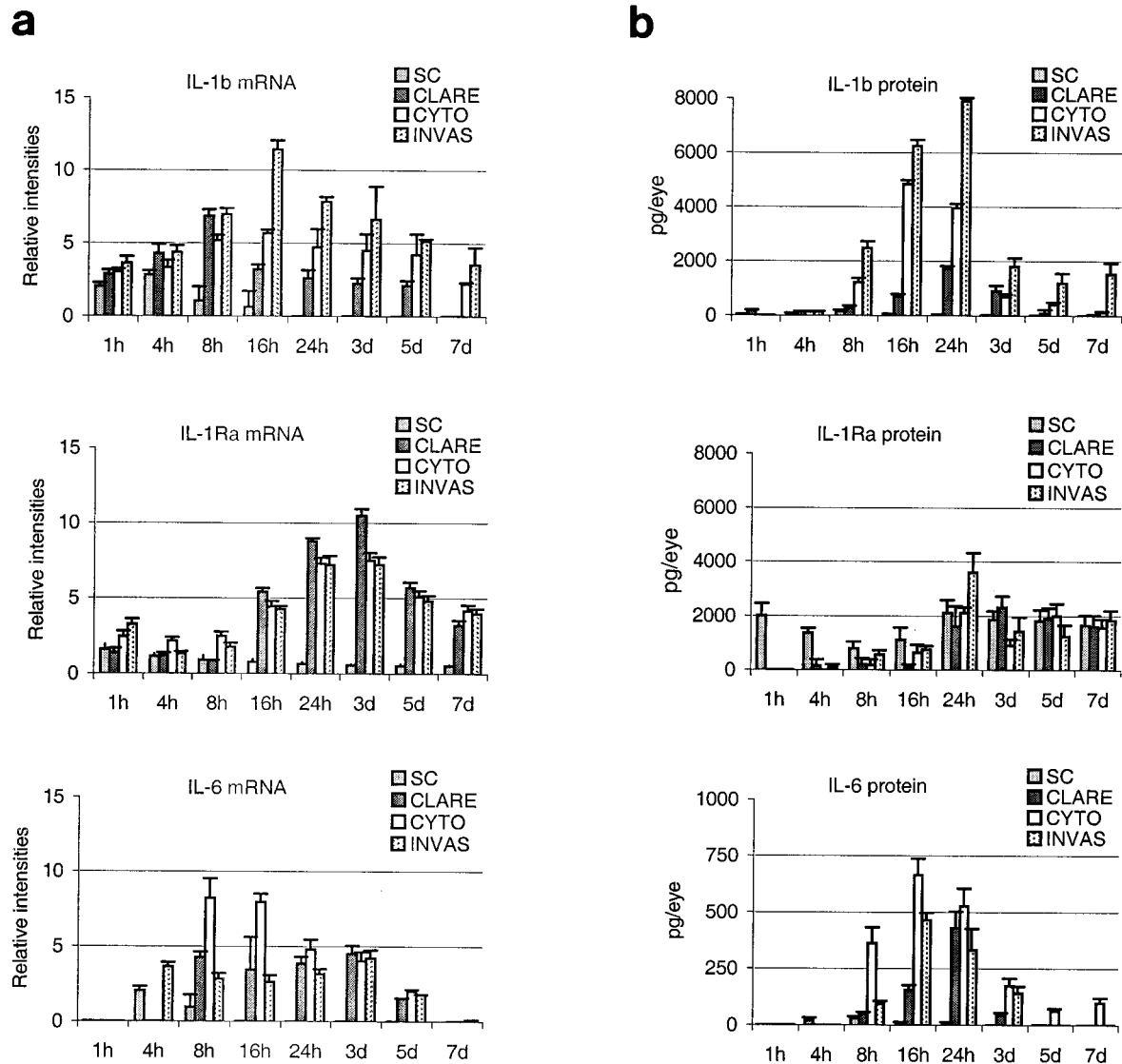
a

b

FIG. 4. (a) Time-dependent expression of cytokine mRNAs in mouse corneas at 1, 4, 8, 16, and 24 h and 3, 5, and 7 days postchallenge with the invasive (INVAS), cytotoxic (CYTO), or CLARE bacterial strain. Results are presented as the mean ($\pm$ standard error of the mean) relative intensity of each cytokine band divided by the intensity of the respective GAPDH band in the same lane. (b) Time dependent expression of cytokine proteins in mouse corneas at 1, 4, 8, 16, and 24 h and 3, 5, and 7 days postchallenge with the invasive, cytotoxic, or CLARE bacterial strain. Results are presented as mean ($\pm$ standard error of the mean) picograms of cytokine protein/eye. Note that the horizontal axis is not on a linear scale. SC, scratch control.

24 h postchallenge, declined markedly on day 3, and then remained static until day 7 postchallenge. A similar pattern was followed by the IL-1Ra and IL-6 proteins (Fig. 4b). Consistent with mRNA expression, only very low levels of TNF-α and IL-10 proteins were detected in response to all three bacterial strains (data not shown).

Ocular IL-1β/IL-1Ra ratios correlate with severity of corneal disease. IL-1β/IL-1Ra ratios in response to the three strains of *P. aeruginosa* were compared at 1, 3, 5, and 7 days. Corneas challenged with the invasive strain showed significantly lower ratios of IL-1Ra/IL-1β at all time points (1, 3, 5, and 7 days) than either the cytotoxic or CLARE strain. A significant correlation was found between the IL-1Ra/IL-1β ratio and the severity of corneal disease judged by the com-

posite corneal scores ($r = -0.65$; $P < 0.02$) and between this ratio and corneal neovascularization ($r = -0.95$; $P < 0.046$). Correlations between the levels of IL-6 and the composite corneal scores (stromal infiltrates and epithelial defect), corneal edema, and neovascularization were also sought. There was no significant correlation found between the levels of IL-6 and any of the variables of the corneal disease. However, there appeared to be a strong trend suggesting that initial higher levels of IL-6 may lead to faster resolution of corneal disease. The results are presented in Tables 2 and 3.

Administration of mouse rIL-1Ra reduces disease severity. Mice were injected with 20 μg of rIL-1Ra or PBS (controls) subconjunctivally at 24 h and then 3 h before infection with the invasive strain of *P. aeruginosa*. Clinical examination was per-

TABLE 2. Comparison of composite corneal scores (CS) (corneal infiltrates and epithelial defects), edema (E), and neovascularization (NV) with IL-1Ra/IL-1β ratio in corneas of mice infected with three strains of *P. aeruginosa*[a]

Time postinfection (days)	Invasive strain				Cytotoxic strain				CLARE strain			
	CS[b]	E	NV[b]	IL-1Ra/IL-1β ratio	CS[b]	E	NV[b]	IL-1Ra/IL-1β ratio	CS[b]	E	NV[b]	IL-1Ra/IL-1β ratio
1	14.7 ± 2	0 ± 0	0 ± 0	0.45	9.4 ± 5.0	2.5 ± 0.5	0 ± 0	0.5	5 ± 1	0 ± 0	0 ± 0	1.06
3	12.5 ± 7	3.5 ± 0.5	0.2 ± 0.06	0.75	8.3 ± 0.9	2.0 ± 0.5	0.1 ± 0.07	1.3	0 ± 0	0 ± 0	0 ± 0	2.5
5	11.5 ± 5	3.2 ± 0.8	0.6 ± 0.1	0.8	6.8 ± 0.7	1.2 ± 1.0	0 ± 0	5	0 ± 0	0 ± 0	0 ± 0	21
7	8 ± 3	0.8 ± 0.8	1.2 ± 0.3	1.5	5.4 ± 0.8	0 ± 0	0 ± 0	11	0 ± 0	0 ± 0	0 ± 0	40

[a] CS, E, and NV values are means ± standard deviations.
[b] $P < 0.05$.

formed on days 1, 3, and 7 postchallenge; following clinical examination, eyes were enucleated and processed for histological examination and PMN infiltration.

Clinical and histological examination. Clinical and histological examinations were performed on days 1, 3, and 7 postchallenge (these time points were selected because maximum severity was present at 1 to 3 days postchallenge and the severity declined significantly by day 7) in mice that received rIL-1Ra protein subconjunctivally at 24 and 3 h before infection with invasive strain. The third control group received rIL-1Ra injection but was not infected. Mice treated with rIL-1Ra before the infection showed few focal infiltrates at the periphery of the cornea compared to PBS-treated infected controls, which showed massive infiltrates in the central cornea with severe edema at 1 day postchallenge. The composite clinical scores were significantly ($P < 0.001$) reduced in mice that received rIL-1Ra protein (6.6 ± 1.2) compared to those that received PBS (14.7 ± 2.2) before infection with the invasive strain at 1 day postchallenge. In mice treated with rIL-1Ra, corneas appeared normal on day 7 compared to those of PBS-treated (7.9 ± 2.5) mice (Fig. 5). rIL-1Ra-injected uninfected controls did not show any sign of inflammation at 1 day postinjection, and therefore these data are not presented.

Histological examination also showed noticeably reduced cellular infiltration in mice that received rIL-1Ra protein (Fig. 6A) compared to those that received PBS (control) before infection at 1 day postchallenge. Control animals showed massive infiltration of inflammatory cells in the corneal stroma as well as in the anterior chamber, with severe edema and destruction of the corneal epithelium in the central cornea (Fig. 6B). On day 7, infiltrating cells could not be seen in the corneal stroma of mice that received rIL-1Ra protein (Fig. 6C). Control animals those that received PBS (Fig. 6D) still had large numbers of infiltrates although corneal epithelium had healed, but neovascularization was evident in the corneal stroma.

PMN infiltration. PMN numbers were quantitated by measuring the MPO activity of the eye in mice treated with rIL-1Ra protein and compared with those for control untreated mice. MPO activity was significantly ($P < 0.004$) reduced in IL-1Ra-treated mice compared to control mice at 1 day postchallenge. On day 7, MPO activity reached baseline levels in rIL-1Ra-treated mice compared to controls. These results are presented in Fig. 7.

DISCUSSION

This study has demonstrated that the severity of corneal disease during *P. aeruginosa* infection correlates with the ratio of IL-1Ra to IL-1β and that exogenous administration of rIL-1Ra is able to reduce the disease severity significantly. The levels of IL-1β, IL-6, and IL-1Ra and the kinetics of appearance were different in corneas challenged with strains that produce distinct pathologies. In response to challenge with the invasive strain, levels of IL-1Ra were initially (at 1 to 8 h) down-regulated (compared to those in normal cornea) but rose significantly by 24 h postchallenge. IL-1Ra is a naturally occurring IL-1 isoform typically produced by the same cells that synthesize IL-1. IL-1Ra binds IL-1 receptors with high affinity but shows no agonist activity. The ratio of IL-1Ra to IL-1β was significantly correlated (inversely) with the severity of corneal disease and neovascularization. These findings suggest that high levels of IL-1Ra or a higher IL-1Ra/IL-1β ratio are associated with reduced inflammation. Previous studies have shown that only a 10-fold excess of IL-1Ra over IL-1 completely inhibited IL-1-induced responses in human hepatoma cells (6). On the other hand, the synovial fluid IL-1Ra/IL-1β ratio in Lyme arthritis exceeded 50 in patients with fast recovery, whereas the ratio was less than 30 in those with prolonged illness (38). In experimental endotoxemia, a 100-fold molar excess of IL-1Ra over IL-1β was required to block *Escherichia*

TABLE 3. Comparison of composite corneal scores (CS) (corneal infiltrates and epithelial defects), edema (E), and neovascularization (NV) with IL-6 protein levels in corneas of mice infected with three strains of *P. aeruginosa*[a]

Time postinfection (days)	Invasive strain				Cytotoxic strain				CLARE strain			
	CS	E	NV	IL-6 (pg/ml)	CS	E	NV	IL-6 (pg/ml)	CS	E	NV	IL-6 (pg/ml)
1	14.7 ± 2§	0 ± 0	0 ± 0	320	9.4 ± 5.0	2.5 ± 0.5	0 ± 0	510	5 ± 1	0 ± 0	0 ± 0	425
3	12.5 ± 7	3.5 ± 0.5	0.2 ± 0.06	125	8.3 ± 0.9	2.0 ± 0.5	0.1 ± 0.07	175	0 ± 0	0 ± 0	0 ± 0	65
5	11.5 ± 5	3.2 ± 0.8	0.6 ± 0.1	0	6.8 ± 0.7	1.2 ± 1.0	0 ± 0	75	0 ± 0	0 ± 0	0 ± 0	0
7	8 ± 3	0.8 ± 0.8	1.2 ± 0.3	0	5.4 ± 0.8	0 ± 0	0 ± 0	100	0 ± 0	0 ± 0	0 ± 0	0

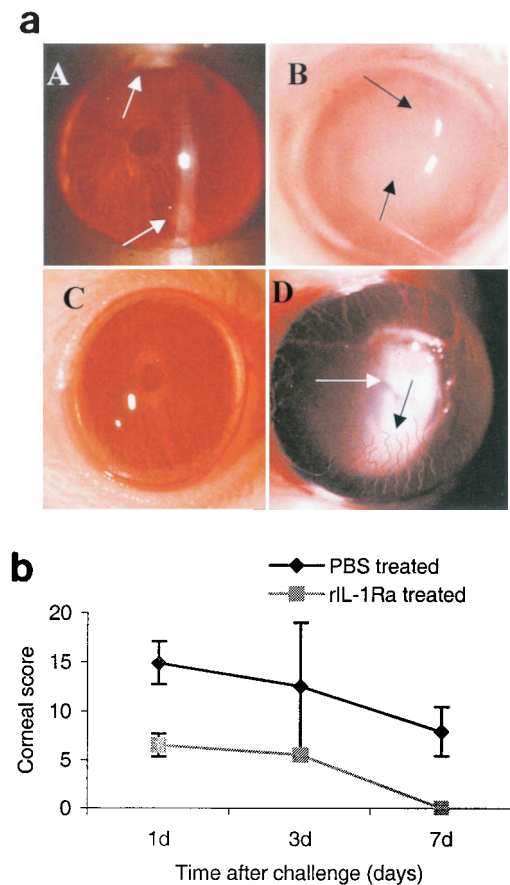[a] CS, E, and NV values are means ± standard deviations.

a

b

FIG. 5. (a) Clinical examination of corneas injected with 20 μl of rIL-1Ra (20 μg during each injection) subconjunctivally at 24 h and then 3 h before infection with the invasive strain. Control mice received an equal volume of PBS at same time points before the infection with invasive strain. Panel A, rIL-1Ra-treated mice at 24 h postchallenge, showing focal infiltrates at the periphery of the cornea (arrows). Panel B, control mice showed extensive infiltration of inflammatory cells (arrow) in the central cornea at 24 h postchallenge, with severe edema and moderate anterior chamber response. Panel C, rIL-1Ra-treated mice at 7 days postchallenge; infiltrates have completely resolved. Panel D, in control mice the epithelium had healed but a large number of infiltrates were still present (white arrow), and new vessel growth was evident (black arrow). (b) Composite clinical scores (composed of the graded density, depth, and extent of corneal infiltrates as well as size and depth of corneal ulceration; see Table 1 for the grading system) at 1, 3, and 7 days postchallenge for corneas treated with 20 μl of rIL-1Ra (20 μg during each injection) subconjunctivally at 24 and 3 h before the infection with invasive strain. Control mice received an equal volume of PBS at same time points before the infection with invasive strain. Error bars indicate standard errors of the means.

coli-induced septic shock in rabbits (39). The protein assay used in the present study measured only free IL-1Ra, and hence the total concentration of IL-1Ra (bound plus free) in the ocular samples is not known.

The presence of IL-1β protein has been correlated with the severity of various ocular inflammation models, including herpes simplex virus-induced corneal infection (57) and corneal allograft rejection (13). The precise role played by IL-1β in the cornea in response to *P. aeruginosa* infection is not clear. IL-1β is a potent proinflammatory cytokine and is involved in the

effector phase of inflammatory and immune responses, including activation of the phagocytic and killing capacities of inflammatory cells, as well as up-regulation and activation of vascular adhesion molecules (36, 41) such as ICAM-1. In addition, IL-1β can induce IL-8 and GROα (neutrophil-attracting chemokines) in many cell types to facilitate recruitment of PMNs into the cornea (4, 48). In addition to facilitating bacterial clearance, PMNs are thought to play a crucial role in tissue damage via activation of matrix metalloproteinases (40). Local release and enhanced production of IL-1β by infiltrating cells in the bacterial keratitis model may amplify the process of PMN accumulation. Rudner et al. (45) have recently shown that neutralization of IL-1β activity can reduce the severity of corneal disease by down-regulating macrophage-inhibitory protein 2(MIP-2) expression during murine keratitis induced by a cytotoxic strain of *P. aeruginosa* (strain 19660).

In response to both the invasive and cytotoxic strains, prominent ulceration was evident in conjunction with high levels of IL-1β. IL-1β has been shown to induce expression of matrix metalloproteinases (MMPs) in diverse cell culture systems, including up-regulation of MMP-1 and MMP-3 in fibroblasts isolated from corneal stromal (24), gingival (54), synovial (35), colon (5), and endometrial stromal (42) cells. A more recent study has shown IL-1β-induced up-regulation of MMPs in fibroblasts isolated from conjunctiva (37). MMPs have also been implicated in pathological tissue degradation in inflammatory diseases of the eye, notably uveitis and scleritis (14–16). The mechanism of host-mediated corneal destruction is not clear; we propose that IL-1β induces expression and activation of MMPs in both infiltrating PMNs and resident corneal cells, leading to an imbalance in the level of MMPs and tissue inhibitors of MMPs resulting in significant corneal tissue destruction.

IL-1β is also a potent inducer of angiogenic factors such as IL-8 (the human counterpart of murine MIP-2/KC) and vascular endothelial growth factor (VEGF) (34, 1). Recent studies have implicated VEGF and bovine fibroblast growth factor in the development of iris and retinal neovascularization (3). In addition, Yoshida et al. (58) have shown that IL-8 participates in the pathogenesis of retinal neovascularization through activation of NF-κB. In the present study, a significant correlation between the ratio of IL-1Ra/IL-1β and the extent of new vessel growth in the cornea was found, suggesting direct involvement of IL-1β in the process of angiogenesis.

IL-6 was significantly up-regulated in response to the cytotoxic and CLARE strains and to a lesser extent in response to the invasive strain. IL-6 is generally regarded as sharing overlapping functions with IL-1 and TNF (2), such as activation of inflammatory cells and up-regulation of adhesion molecules. On the other hand, IL-6 can also function as an anti-inflammatory cytokine by down-regulating the production of IL-1 and TNF (46). A recent study has also demonstrated that IL-6 can induce synthesis of IL-1Ra (53). In the present study, early up-regulation of IL-6 was associated with less severe corneal inflammation. This finding is consistent with a previous report that IL-6-deficient mice had increased bacterial loads during infection with *Listeria monocytogenes* (12).

Corneal damage is also likely to be attributed to the ability of each *Pseudomonas* strain to produce proteolytic enzymes, i.e., LasB elastase, LasA protease, alkaline protease, and pro-
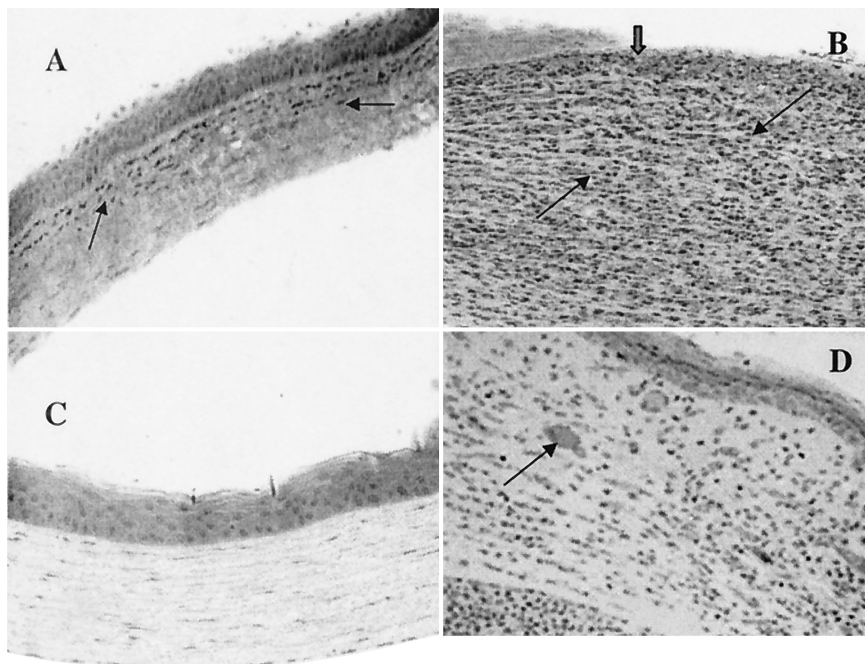
FIG. 6. Animals were injected with 20 μl of rIL-1Ra (20 μg during each injection) subconjunctivally at 24 h and then 3 h before infection with the invasive strain. Control mice received an equal volume of PBS at same time points before the infection with invasive strain. (A) Histological examination showed fewer infiltrates in the anterior stroma (arrow) and no epithelial defect at 1 day postchallenge in the corneas treated with rIL-1Ra protein. (B) Control mice had enormous infiltrates (thin black arrows) with complete loss of epithelium in the central cornea (thick arrow) at 1 day postchallenge. (C) In rIL-1Ra-treated mice, corneas were completely recovered by day 7 postchallenge. (D) In control mice, infiltrates have reduced compared to those at 1 day postchallenge and epithelium has healed (thick arrow) in the central cornea. Neovascularization is evident in the corneal stroma (arrow).

tease IV (25, 26). Both the cytotoxic and invasive strains have been shown to produce large number of proteinases (10, 22). By contrast, the CLARE phenotype is neither invasive nor cytotoxic and has been shown to produce low levels of proteinases (10, 18). Previous studies with *Pseudomonas* strains have demonstrated that cytokine production in vivo is correlated to a large extent with the virulence of the pathogen (17, 27). Consistent with these studies, the three strains used in this study differed significantly in the kinetics and magnitude of cytokine induction. A recent study has shown that exoenzyme S (present in the invasive strain, a highly virulent strain) can rapidly induce various cytokines (IL-1α, IL-1β, and IL-6) in host cells (17). The cytotoxic strain used in the present study lacks the *exoS* gene (19). It appears likely that the greater magnitude of the cytokine responses produced by the invasive strain may be related to the capability of key virulence factors in the microorganism to induce cytokine production in the host. It is possible that the effects observed on progression of disease and cytokine responses by the three bacterial strains demonstrate either responses to the bacterial phenotypes in general or responses to the bacterial strains in particular. This was not investigated in the present study, and the use of isogenic mutants would be required to study this in detail. However, Kernacki et al. (33) show a clinical picture of another cytotoxic strain, strain 19660, that is remarkably similar to the clinical disease caused by our cytotoxic strain, 6206. Both strains appear to produce a ring infiltrative response in BALB/c mice (33) (Fig. 1a, panel d). Also, we have tested the ability of two other invasive strains of *P. aeruginosa* (Paer24

and Paer25, isolated from contact lens wearers at the Cooperative Research Centre for Eye Research and Technology) to produce disease in BALB/c mice, and these show clinical and histological corneal responses (unpublished data) very similar to those seen with the invasive strain used in this study.

Based on our findings, we speculate that continued up-regulation of IL-1β, down-regulation of IL-1Ra, and relatively low levels of induction of IL-6 are the major factors contributing to severe corneal disease induced by *Pseudomonas* strains. The balance between pro- and anti-inflammatory cytokines appar-
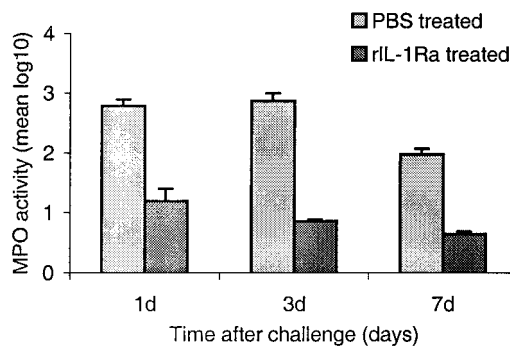

FIG. 7. MPO activity in rIL-1Ra-treated and control (PBS-treated) mouse eyes challenged with the invasive strain at 1, 3, and 7 days postchallenge. Results are reported as mean (± standard error of the mean) $\log_{10}$ MPO activity/eye. Note that the horizontal axis is not on a linear scale.

ently determines the net effect of the inflammatory response in this model. Administration of rIL-1Ra significantly reduced disease severity. Therapies based on better understanding of these host-pathogen interactions may help save vision in severe bacterial keratitis.

REFERENCES

1. **Aiello, L. P., E. A. Pierce, and E. D. Foley.** 1995. Suppression of retinal neovascularization in vivo by inhibition of VEGF using soluble VEGF receptor chimeric proteins. Proc. Natl. Acad. Sci. USA **92:**10457–10461.
2. **Akira, S., T. Hirano, T. Taga, and T. Kishimoto.** 1990. Biology of multifunctional cytokines: IL 6 and related molecules (IL 1 and TNF). FASEB J. **4:**2860–2867.
3. **Amano, S., R. Rohan, and M. Kuroki.** 1998. Requirement for VEGF in wound and inflammation related corneal neovascularization. Investig. Ophthalmol. Vis. Sci. **39:**18–22.
4. **Anisowicz, A., M. Messineo, S. W. Lee, and R. Sager.** 1991. NF-κB-like transcription factor mediates IL-1/TNF-α induction of GRO in human fibroblasts. J. Immunol. **147:**520–527.
5. **Baugh, M. D., A. P. Hollander, and G. S. Evans.** 1998. The regulation of matrix metalloproteinase production in human colonic fibroblasts. Ann. N.Y. Acad. Sci. **859:**175–179.
6. **Bevan, S., and J. G. Raynes.** 1991. IL-1 receptor antagonist regulation of acute phase protein synthesis in human hepatoma cells. J. Immunol. **147:**2574–2578.
7. **Chusid, M. J., and S. D. Davis.** 1979. Experimental bacterial keratitis in neutropenic guinea pigs: polymorphonuclear leukocytes in corneal host defense. Infect. Immun. **24:**948–952.
8. **Cole, N., S. Bao, M. Willcox, and A. J. Husband.** 1999. Expression of interleukin-6 in the cornea in response to infection with different strains of *Pseudomonas aeruginosa.* Infect. Immun. **67:**2497–2502.
9. **Cole, N., M. D. P. Willcox, S. M. J., Fleiszig, F. Stapleton, S. Bao, S. Tout, and A. Husband.** 1998. Different strains of *Pseudomonas aeruginosa* isolated from ocular infections or inflammation display distinct corneal pathologies in an animal model. Curr. Eye Res. **17:**730–735.
10. **Cowell, B. A., M. D. P. Willcox, J. A. Hobden, R. P. Schneider, S. Tout, and L. D. Hazlett.** 1998. An ocular strain of *Pseudomonas aeruginosa* is inflammatory but not virulent in the scarified mouse model. Exp. Eye Res. **67:**347–356.
11. **Cubitt, C. L., R. N. Lausch, and J. E. Oakes.** 1995. Differences in IL-6 gene expression between cultured human corneal epithelial cells and keratocytes. Investig. Ophthalmol. Vis. Sci. **36:**330–336.
12. **Dalrymple, S. A., L. A. Lucian, R. Slattery, T. McNeil, D. M. Aud, S. Fuchino, F. Lee, and F. Murray.** 1995. Interleukin-6-deficient mice are highly susceptible to *Listeria monocytogenes* infection: correlation with inefficient neutrophilia. Infect. Immun. **63:**2262–2268.
13. **Dana, M. R., J. Yamada, and J. W. Streilein.** 1997. Topical interleukin 1 receptor antagonist promotes corneal transplant survival. Transplantation **63:**1501–1507.
14. **Di Girolamo, N., M. J. Verma, P. J. McCluskey, A. Lloyd, and D. Wakefield.** 1996. Increased matrix metalloproteinases in the aqueous humor of patients and experimental animals with uveitis. Curr. Eye Res. **10:**1060.
15. **Di Girolamo, N., A. Lloyd, P. McCluskey, M. Filipic, and D. Wakefield.** 1997. Increased expression of matrix metalloproteinases in vivo in scleritis tissue and in vitro in cultured human scleral fibroblasts. Am. J. Pathol. **150:**653–666.
16. **Di Girolamo, N., P. McCluskey, A. Lloyd, M. T. Coroneo, and D. Wakefield.** 2000. Expression of MMPs and TIMPs in human pterygia and cultured pterygium epithelial cells. Investig. Ophthalmol. Vis. Sci. **41:**671–679.
17. **Epelman, S., T. F. Bruno, G. G. Neely, D. E. Woods, and C. H. Mody.** 2000. *Pseudomonas aeruginosa* exoenzyme S induces transcriptional expression of proinflammatory cytokines and chemokines. Infect. Immun. **68:**4811–4814.
18. **Estrellas, P. S., Jr., L. G. Alionte, and J. A. Hobden.** 2000. A Pseudomonas aeruginosa strain isolated from a contact lens-induced acute red eye (CLARE) is protease-deficient. Curr Eye Res. **20:**157–165.
19. **Finck-Barbancon, V., J. Goranson, L. Zhi, T. Sawa, J. P. Wiener-Kronish, S. M. J. Fleiszig, C. Wu, L. Mende-Mueller, and D. W. Frank.** 1997. ExoU expression by *Pseudomonas aeruginosa* correlates with acute cytotoxicity and epithelial injury. Mol. Microbiol. **25:**547–557.
20. **Fleiszig, S. M. J., J. P. Wiener-Kronish, V. Miyazaki, V. Vallas, K. E. Mastov, D. Kanada, T. Sawa, T. S. B. Yen, and D. W. Frank.** 1997. *Pseudomonas aeruginosa*-mediated cytotoxicity and invasion correlate with distinct genotype at the loci encoding exoenzyme S. Infect. Immun. **65:**579–586.
21. **Fleiszig, S. M., T. S. Zaidi, E. L. Fletcher, M. J. Preston, and G. B. Pier.** 1994. *Pseudomonas aeruginosa* invades corneal epithelial cells during experimental infection. Infect. Immun. **62:**3485–3493.
22. **Fleiszig, S. M., T. S. Zaidi, and G. B. Pier.** 1995. *Pseudomonas aeruginosa* invasion of and multiplication within corneal epithelial cells in vitro. Infect. Immun. **63:**4072–4077.
23. **Fleiszig, S. M., T. S. Zaidi, M. J. Preston, M. Grout, D. J. Evans, and G. B. Pier.** 1996. Relationship between cytotoxicity and corneal epithelial cell invasion by clinical isolates of *Pseudomonas aeruginosa*. Infect. Immun. **64:**2288–2294.
24. **Girard, M. T., M. Matsubara, and M. E. Fini.** 1991. Transforming growth factor β and interleukin-1 modulate metalloproteinases expression by corneal stromal cells. Investig. Ophthalmol. Vis. Sci. **32:**2441–2454.
25. **Heck, L. W., K. Morihara, and D. R. Abrahamson.** 1986. Degradation of soluble laminin and depletion of tissue-associated basement membrane laminin by *Pseudomonas aeruginosa* elastase and alkaline protease. Infect. Immun. **54:**149–153.
26. **Heck, L. W., K. Morihara, W. B. McRae, and E. J. Miller.** 1986. Specific cleavage of human type III and IV collagens by *Pseudomonas aeruginosa* elastase. Infect. Immun. **51:**115–118.
27. **Hirakata, Y., T. Kirikae, F. Kirikae, T. Yamaguchi, K. Izumikawa, H. Takemura, K. Maesaki, K. Tomono, Y. Yamada, S. Kamihira, M. Nakano, and S. Kitamura.** 1999. Effect of *Pseudomonas aeruginosa* exotoxin A on endotoxin-induced tumour necrosis factor production in murine lung . J. Med. Microbiol. **48:**471–477.
28. **Hobden, J. A., S. A. Masinick, R. P. Barret, and L. D. Hazlett.** 1997. Proinflammatory cytokine deficiency and pathogenesis of *Pseudomonas aeruginosa* keratitis in aged mice. Infect. Immun. **65:**2754–2758.
29. **Kernacki, K. A., and R. S. Berk.** 1994. Characterization of the inflammatory response induced by corneal infection induced by *Pseudomonas aeruginosa*. J. Ocular Pharmacol. **10:**281.
30. **Kernacki, K. A., J. A. Hobden, L. D. Hazlett, R. Fridman, and R. S. Berk.** 1995. In vivo bacterial protease production during *Pseudomonas aeruginosa* corneal infection. Investig. Ophthalmol. Vis. Sci. **36:**1371–1378.
31. **Kernacki, K. A., R. Fridman, L. D. Hazlett, M. A. Lande, and R. S. Berk.** 1997. In vivo characterization of host and bacterial protease expression during *Pseudomonas aeruginosa* corneal infections in naive and immunized mice. Curr. Eye Res. **16:**289–297.
32. **Kernacki, K. A., D. J. Goebel, M. S. Poosch, and L. D. Hazlett.** 1998. Early cytokine and chemokine gene expression during *Pseudomonas aeruginosa* corneal infection in mice. Infect. Immun. **66:**376–379.
33. **Kernacki, K. A., R. Barrett, and L. D. Hazlett.** 1999. Evidence for TIMP-1 protection against *P. aeruginosa*-induced corneal ulceration and perforation. Investig. Ophthalmol. Vis. Sci. **40:**3168–3176.
34. **Li, J., N. Yoshikawa, and D. T. Connolly.** 1995. Induction of vascular endothelial growth factor gene expression by IL-1 beta in rat aortic smooth muscle cells. J. Biol. Chem. **270:**308–312.
35. **MacNaul, K. L., N. Chartrain, M. Lark, M. J. Tocci, and N. I. Hutchinson.** 1990. Discoordinate expression of stromelysin, collagenase, and tissue inhibitor of metalloproteinases-1 in rheumatoid human synovial fibroblasts. Synergistic effects of interleukin-1 and tumor necrosis factor-alpha on stromelysin expression. J. Biol. Chem. **265:**17238–17245.
36. **Meager, A.** 1999. Cytokine regulation of cellular adhesion molecule expression in inflammation. Cytokine Growth Factor Rev. **10:**27–39.
37. **Meller, D., D. Q. Li, and S. C. Tseng.** 2000. Regulation of collagenase, stromelysin, and gelatinase B in human conjunctival and conjunctivochalasis fibroblasts by interleukin-1beta and tumor necrosis factor-alpha. Investig. Ophthalmol. Vis. Sci. **41:**2922–2929.
38. **Miller, L. C., E. A. Lynch, and S. Isa.** 1993. Balance of synovial fluid IL-1β and IL-1 receptor antagonist and recovery from Lyme arthritis. Lancet **341:**146–148.
39. **Ohlsson, K., P. Bjork, M. Bergenfeldt, and R. Hageman.** 1990. Thompson RC interleukin-1 receptor antagonist reduces mortality from endotoxin shock. Nature **348:**550–552.
40. **Okada, Y., and I. Nakanishi.** 1989. Activation of matrix metalloproteinase 3 (stromelysin) and matrix metalloproteinase 2 ('gelatinase') by human neutrophil elastase and cathepsin G. FEBS Lett. **249:**353–356.
41. **Pavilack, M. A., V. M. Elner, S. G. Elner, R. F. Todd, and A. R. Huber.** 1992. Differential expression of human corneal and prelimbal ICAM-1 by inflammatory cytokines. Invest. Ophthalmol. Vis. Sci. **33:**564–573.
42. **Rawdanowicz, T. J., A. L. Hampton, H. Nagase, D. E. Woolley, and L. A. Salamonsen.** 1994. Matrix metalloproteinase production by cultured human endometrial stromal cells: identification of interstitial collagenase, gelatinase-A, gelatinase-B, and stromelysin-1 and their differential regulation by interleukin-1α and tumor necrosis factor-α. J. Clin. Endocrinol. Metab. **79:**530–536.
43. **Ries, C., and P. E. Pertrides.** 1995. Cytokine regulation of matrix metallo-

proteinases activity and its regulatory dysfunction in disease. J. Biol. Chem. **376:**345–355.

44. **Rosenbaum, J. T., S. R. Planck, and X. N. Huang.** 1995. Detection of mRNA for the cytokines IL-1α and IL-8 in corneas from patients with pseudophakic bullous keratopathy. Investig. Ophthalmol. Vis. Sci. **36:**2151–2155.

45. **Rudner, X. L., K. A. Kernacki, R. P. Barrett, and L. D. Hazlett.** 2000. Prolonged elevation of IL-1 in *Pseudomonas aeruginosa* ocular infection regulates macrophage-inflammatory protein-2 production, polymorphonuclear neutrophil persistence, and corneal perforation. J. Immunol. **164:**6576–6582.

46. **Schindler, R., J. Mancilla, S. Endres, R. Ghorbani, S. C. Clark, and C. A. Dinarello.** 1990. Correlations and interactions in the production of IL-6, IL-1 and TNF in human blood mononuclear cells: IL-6 suppresses IL-1 and TNF. Blood **75:**40–47.

47. **Steuhl, K. P., G. Doring, and H. J. Theil.** 1989. The significance of bacterial and host factors in corneal infections caused by *Pseudomonas aeruginosa*. Fortschr. Ophthalmol. **86:**283.

48. **Stoeckle, M. Y.** 1991. Post-transcriptional regulation of GROα, β, γ and IL-8 mRNAs by IL-1β. Nucleic Acids Res. **19:**917–920.

49. **Thakur, A., and M. D. P. Willcox.** 1998. Chemotactic activity in tears and bacteria isolated during contact lens induced adverse events. Exp. Eye Res. **66:**129–137.

50. **Thakur, A., M. D. P. Willcox, and F. Stapleton.** 1998. The proinflammatory cytokines and arachidonic acid metabolites in human tears: homeostatic mechanism. J. Clin. Immunol. **18:**61–70.

51. **Thakur, A., and M. D. P. Willcox.** 1998. Cytokines and lipid inflammatory mediator profile of human tears of contact lens associated inflammatory diseases. Exp. Eye Res. **67:**9–19.

52. **Thiel, H. J., K. P. Steuhl, and G. Doring.** 1987. Therapy of *Pseudomonas aeruginosa* eye infections. Antibiot. Chemother. **39:**92–101.

53. **Tilg, H., E. Trehu, M. B. Athins, C. A. Dinarello, and J. W. Mier.** 1994. Interleukin-6 as an anti-inflammatory cytokine: induction of circulation IL-1 receptor antagonist and soluble tumor necrosis factor receptor p55. Blood **83:**113–118.

54. **Wassenaar, A., T. Verschoor, F. Kievits, M. T. Den Hartog, M. L. Kapsenberg, V. Everts, and A. Snijders.** 1999. CD40 engagement modulates the production of matrix metalloproteinases by gingival fibroblasts. Clin. Exp. Immunol. **115:**161–167.

55. **Weiss, S. J.** 1989. Tissue destruction by neutrophils. N. Engl. J. Med. **320:**365–376.

56. **Williams, R. N., C. A. Patterson, and K. E. Eakins.** 1983. Quantitation of ocular inflammation: evaluation of polymorphonuclear leukocyte inflammation by measuring myeloperoxidase activity. Curr. Eye Res. **2:**465–470.

57. **Yan, X. T., T. M. Tumpey, S. L. Kunkel, J. E. Oakes, and R. N. Lausch.** 1998. Role of MIP-2 in neutrophil migration and tissue injury in the herpes simplex virus-1-infected cornea. Investig. Ophthalmol. Vis. Sci. **39:**1854–1862.

58. **Yoshida, A., S. Yoshida, and A. Khalil.** 1998. Role of NF-κB mediated IL-8 expression in intraocular neovascularization. Investig. Ophthalmol. Vis. Sci. **39:**1097–1106.

Editor: J. D. Clements